Arch. Metall. Mater. **67** (2022), 4, 1487-1490

DOI: https://doi.org/10.24425/amm.2022.141079

DONG-KYU OH[1], SEUNG-HYEOK SHIN[1], SANG-MIN LEE[2], BYOUNGCHUL HWANG[1*]

EFFECTS OF THE COILING TEMPERATURE AND ANISOTROPY ON THE TENSILE PROPERTIES OF HIGH-STRENGTH API X70 LINEPIPE STEEL

In this study, the effect of the coiling temperature on the tensile properties of API X70 linepipe steel plates is investigated in terms of the microstructure and related anisotropy. Two coiling temperatures are selected to control the microstructure and tensile properties. The API X70 linepipe steels consist mostly of ferritic microstructures such as polygonal ferrite, acicular ferrite, granular bainite, and pearlite irrespective of the coiling temperature. In order to evaluate the anisotropy in the tensile properties, tensile tests in various directions, in this case 0° (rolling direction), 30°, 45° (diagonal direction), 60°, and 90° (transverse direction) are conducted. As the higher coiling temperature, the larger amount of pearlite is formed, resulting in higher strength and better deformability. The steel has higher ductility and lower strength in the rolling direction than in the transverse direction due to the development of γ-fiber, particularly the {111}<112> texture.

Keywords: linepipe steels; anisotropy; tensile property; texture; microstructure

1. Introduction

API (American Petroleum Institute) linepipe steels are required to have relatively high strength so that they can effectively transport natural gas over long distances under high-pressures. Currently, API linepipe steels are increasingly expected to have good deformability characteristics, such as continuous yielding behavior, a low yield-to-tensile ratio, high uniform elongation, and a strain hardening exponent [1-9]. These characteristics are generally used to guarantee resistance to unexpected deformation caused by earthquakes, deep sea conditions, and discontinuous permafrost regions. However, API linepipe steel plates commonly show anisotropy of mechanical properties due to asymmetric deformation during hot rolling [10-12]. In the processes of UOE forming and electric resistance welding (ERW) when manufacturing final linepipe products, API linepipe steels are subjected to different types of deformation depending on the direction. In order to avoid non-uniform deformation and excessive stress in the design of linepipe steels, the anisotropy of API linepipe steels should be considered from the standpoint of structural integrity. On the other hand, recently produced high-strength API linepipe steels are often manufactured through a thermomechanical control process (TMCP) involving controlled rolling and accelerated cooling process to satisfy required properties. During the TMCP, complex microstructures such as polygonal ferrite (PF), quasi-polygonal ferrite (QPF), granular bainitic ferrite (GB), bainitic ferrite (BF), and acicular ferrite (AF) are usually formed with variations in the rolling temperature and cooling rate. Accordingly, it is difficult to measure the anisotropy of tensile properties in relation to the microstructure and to determine the correlation between the microstructure and the tensile properties [13-14]. For API X70 linepipe steel plates fabricated with two coiling temperatures, therefore, the microstructure is characterized by OM, SEM, and EBSD, and the anisotropy of tensile properties such as the yield strength, tensile strength, uniform elongation, and strain hardening exponent is discussed in terms of a crystallographic texture.

2. Experimental

The commercial API X70 grade linepipe steel plates used in this study have the chemical composition of Fe-0.05C-0.16Si-1.1Mn-0.17Cr-0.017Ti-0.056V (wt. %). The steel plate is fabricated by TMCP, with the detailed processing conditions shown in Fig. 1(a). After the finish rolling, the steel plate is cooled and coiled at 570°C and 630°C, respectively. For convenience, these steels are referred to as "CT 570" and "CT 630" according to the coiling temperature (CT). The final thickness of the steel plate

[1] SEOUL NATIONAL UNIVERSITY OF SCIENCE AND TECHNOLOGY, DEPARTMENT OF MATERIALS SCIENCE AND ENGINEERING, SEOUL, 01811, REPUBLIC OF KOREA
[2] HYUNDAI STEEL COMPANY, DANGJIN-SI, CHUNGNAM, 31719, REPUBLIC OF KOREA

* Corresponding author: bhwang@seoultech.ac.kr

is 9.2 mm. The specimens obtained from the rolled steel plates are mechanically polished and etched using a 3% nital solution. The microstructures of the longitudinal-transverse (L-T) plane are observed by a scanning electron microscope (SEM, model; EVO10, Carl Zeiss, Germany). For more detailed microstructure characterization, an electron back-scattered diffraction (EBSD, model; Aztec, Oxford Instruments, UK) analysis is conducted after the specimens are polished using a suspension 0.04 μm colloidal silica particles. The acceleration voltage, working distance, and step size for the EBSD analysis are 15 kV, 11 mm, and 0.18 μm, respectively. The EBSD data is interpreted by Aztec Crystal analysis software (Oxford Instruments, UK).

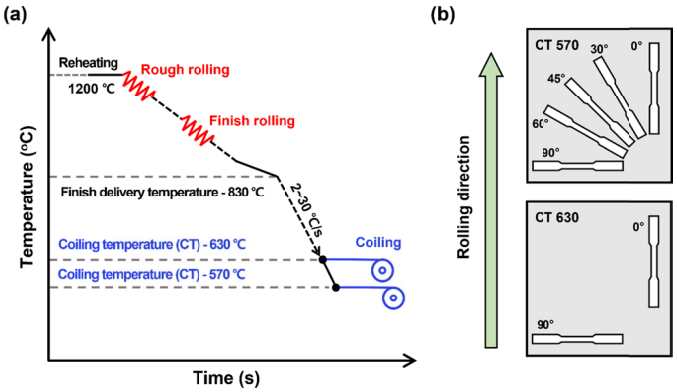

Fig. 1. Schematic illustration showing (a) the thermomechanical control process for the fabrication of the CT 570 and CT 630 steels and (b) the direction of the tensile test specimens

Sub-size plate tensile specimens with a gauge diameter of 6.3 mm and gauge length of 25.0 mm are obtained from the rolled plates in the longitudinal direction. To evaluate the anisotropy of the CT 570 and CT 630 specimens, tensile test specimens are prepared in rolling directions of (0°), 30°, diagonal (45°), 60°, and in the transverse direction (90°) for the CT 570 steel and in the rolling direction of (0°) and in the transverse direction (90°) for the CT 630 steel, as shown in Fig. 1(b). Tensile tests are conducted using a 10-ton universal testing machine (model; UT-100E, MTDI, Korea) according to the ASTM E8 standard test method at room temperature with a crosshead speed of 4.5 mm/min. Stress corresponding to 0.5% strain is determined to be the yield strength of the API linepipe steels [15].

3. Results and discussion

Fig. 2(a) shows SEM micrographs and the EBSD analysis results for the CT 570 and CT 630 steels. As shown in SEM micrographs, both the CT 570 and CT 630 steels exhibit a complex microstructure consisting of polygonal ferrite (PF), acicular ferrite (AF), and granular bainite (GB). The microstructures of API linepipe steels are usually classified according to their transformation behavior and morphological characteristic [16]. The PF has an equiaxed shape with high-angle grain boundaries. Also, the PF has relatively low strength due to its very low dislocation density as it transforms into a fully recrystallized phase at high temperatures and slow cooling rates [17]. The AF is characterized by being aligned with fine and irregular shape grains in random directions, as this type of ferrite is mostly nucleated in deformed austenite bands caused by severe rolling reduction in the non-recrystallized austenite region [18]. Meanwhile, GB contains a sub-grained structure with a large grain size and a coarse island-like martensite-austenite (MA) constituent [19]. In the case of the CT 630 steel, pearlite is additionally formed, due to the relatively high coiling temperature. The PF and AF show a fine grain size, while the GB has coarse grains with many sub-grain boundaries in the CT 570 steel. In addition, the CT 570 steel exhibits the lower fraction of high-angle grain boundaries compared to the CT 630 steel because the lower coiling temperature promotes the formation of microstructures that transform at a low temperature such as AF and GB (Fig. 2(b)).

The room-temperature engineering stress-strain curves of the CT 570 and CT 630 steels are shown in Figs. 3(a,b), and the tensile properties for an average of two or three samples per direction are summarized in TABLE 1. The yield strength and tensile strength of the CT 570 and CT 630 steels meet the

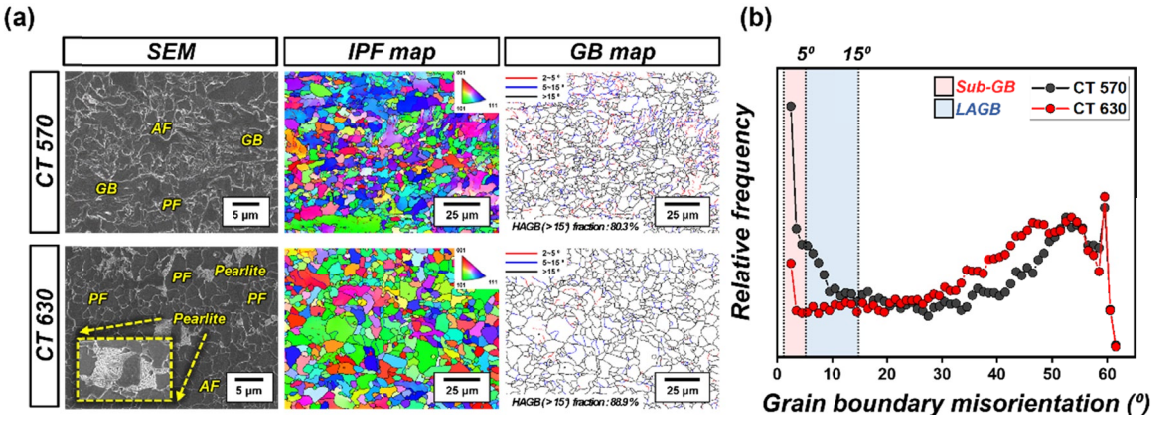

Fig. 2. (a) Scanning electron microscope (SEM) micrographs with marking constituent phases (PF: polygonal ferrite, AF: acicular ferrite, GB: granular bainite, and pearlite), inverse pole figure (IPF), and grain boundary (GB) maps with the high angle grain boundary (HAGB) fractions of the CT 570 and CT 630 steels, and (b) the distribution of grain boundary misorientation with the grain boundaries classified as the sub-grain boundary (Sub-GB) and the low angle grain boundary (LAGB) obtained from electron back-scattered diffraction (EBSD) analysis of the CT 570 and CT 630 steels

API requirements for X70 (485 MPa minimum yield strength and 570 MPa minimum tensile strength) in all directions. The CT 570 and CT 630 steels in all directions show discontinuous yielding behavior because PF is the dominant microstructure in both steels [20-22]. The tensile test data for the CT 630 specimen indicate higher yield strength and tensile strength than the CT 570 specimen at both 0° and 90°. With an increase in the coiling temperature, the yield strength increases by 5.7 MPa and 36.9 MPa, and the tensile strength increases by 18.8 MPa and 18.7 MPa in the 0° and 90° directions, respectively. The tensile strength of high-strength API linepipe steels is typically affected by hard constituent phases such as BF, MA, and pearlite because many dislocations are generated around the grain boundaries between ferrite and the hard phase during deformation [23]. Thus, the yield strength and tensile strength of CT 630 steel are higher than those of CT 570 steel due to the formation of pearlite, a relatively hard microstructure, only in the CT 630 steel. Comparing the uniform elongation at 0°, the CT 630 steel is higher because the fraction of PF increased due to the higher coiling temperature. Lee et al. [24] reported that uniform elongation increased with the fraction of PF in API linepipe steels. The yield strength, tensile strength, uniform elongation, and total elongation variations of the CT 570 and CT 630 steels are shown in Figs. 3(c,d). From variations in the tensile properties results with the specimen direction (Fig. 3(c)), the yield and tensile strength of the CT 570 show relatively low values at 45° and 60°, with the highest at 90°. The uniform elongation and total elongation (Fig. 3(d)), in contrast to the strength, are higher than in the specimens rolled in the directions of 0° and 45°.

According to many studies, anisotropy of tensile properties is mainly observed in rolled steels, especially in body-centered cubic (BCC) materials, and it has been reported to be closely related to texture [25]. In order to understand the anisotropy of tensile properties, therefore, it is important to determine the crystallographic texture and the ideal orientations, which can be observed during the rolling process. Fig. 4 presents a two-dimensional contour map at $\varphi_2 = 45°$ section of the orientation distribution function (ODF) for the CT 570 steel with the main fibers and texture components in rolling. As a result of ODF analysis, the CT 570 presents a low level of α-fiber, whereas a high level of γ-fiber formed by recrystallization, particularly {111}<112> is found, unlike in general plates manufactured by TMCP. This is because the finish delivery temperature (FDT) of

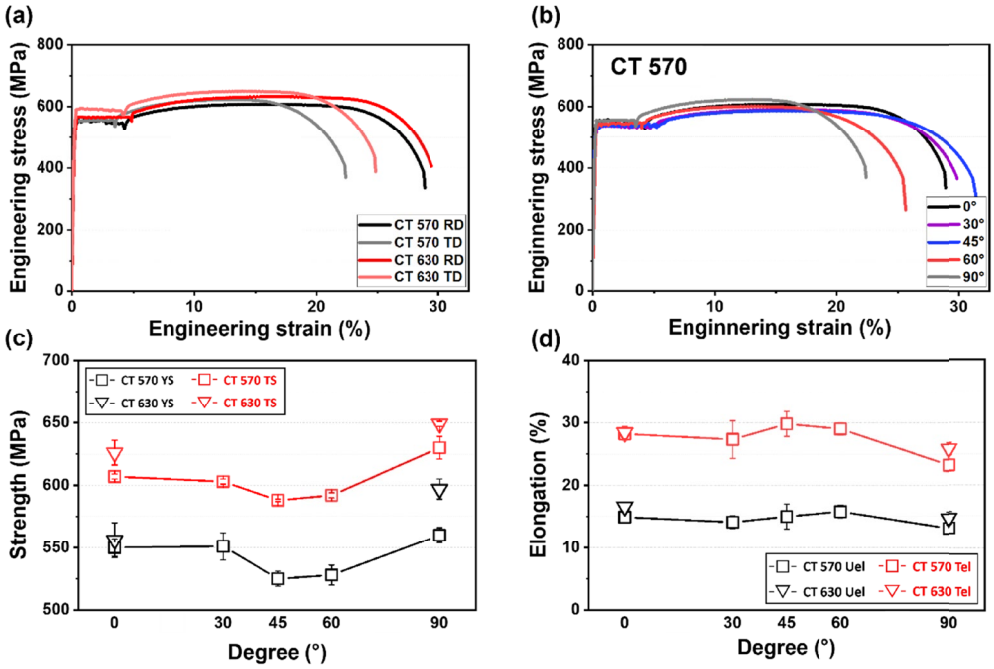

Fig. 3. (a) Engineering stress-strain curves of the rolling and transverse directions for the CT 570 and CT 630 steels; (b) engineering stress-strain curves of the rolling direction (0°), 30°, diagonal (45°), 60°, and transverse (90°) direction for the CT 570 steel; (c) yield and tensile strength; and (d) uniform and total elongations for the CT 570 and CT 630 steels

TABLE 1

Tensile properties in the rolling directions (0°), 30°, diagonal directions (45°), 60°, and transverse direction (90°) for the CT 570 steel and the rolling (0°) and transverse directions (90°) of the CT 630 steel

Specimens	CT 570					CT 630	
	0°	30°	45°	60°	90°	0°	90°
Yield strength (MPa)	550.0±7	551.2±11	524.9±6	528.4±8	560.1±6	555.7±14	597.0±8
Tensile strength (MPa)	607.4±2	603.0±2	588.1±1	592.2±2	630.4±9	626.2±10	649.1±2
Uniform elongation (%)	14.9±0	14.1±1	15.0±2	15.8±1	13.1±0	16.6±0	14.7±1
Total elongation (%)	28.2±1	27.3±3	29.8±2	29.0±1	23.2±1	28.4±1	25.8±1
Yield to tensile strength ratio	0.90±0	0.91±0	0.89±0	0.89±0	0.89±0	0.89±0	0.92±0

the CT 570 is higher than the recrystallization temperature and the stress in the rolling process meets the driving force for recrystallization [26]. Bakshi et al. [27] reported that {111}<112> oriented grains are formed in intercritical range after recrystallization and that they activate slip systems toward the rolling direction resulting in increasing elongation. Therefore, When it comes to the anisotropy of the tensile properties of the CT 570 steel, it can be concluded that {111}<112> oriented grains induce slip in the rolling direction easier, which results in higher ductility and lower strength in the rolling direction than in the transverse direction.

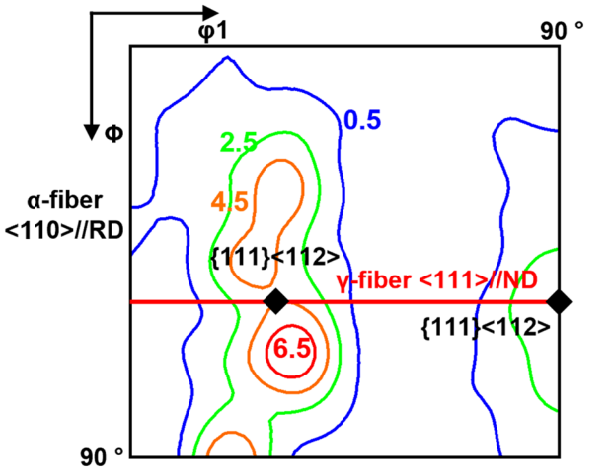

Fig. 4. Two-dimensional contour map at φ_2 = 45° (φ_1 = 0-90° and Φ = 0-90° section) of the orientation distribution function (ODF) from the electron back-scattered diffraction (EBSD) results for the CT 570 steel, indicating the main textures of the steel plates manufactured by TMCP such as α-fiber and γ-fiber

4. Conclusions

1. Low-temperature transformation microstructures such as AF and GB are more frequently observed in the CT 570 steel with a lower coiling temperature, while pearlite is additionally formed in the CT 630 steel due to its relatively high coiling temperature.
2. The yield strength and tensile strength of the CT 630 steel are higher than those of the CT 570 steel due to the formation of pearlite in the CT 630 steel. The CT 630 steel also has relatively high uniform elongation because it contains a larger amount of PF, which is formed by higher coiling temperature.
3. The {111}<112> oriented grains formed by recrystallization activate slip systems and create higher ductility with lower strength in the rolling direction than in the transverse direction.

Acknowledgments

This study was supported by the Technology Innovation Program (Grant No. 20016064) funded by the Ministry of Trade, Industry and Energy (MOTIE), South Korea.

REFERENCES

[1] S.W. Lee, S.I. Lee, B. Hwang, Korean J. Met. Mater. **58**, 293-303 (2020).
[2] N. Amirjani, M. Ketabchi, M. Eskandari, M. Hizombor, Met. Mater. Int. **27**, 4802-4813 (2021).
[3] B. Hamarahi, A. Khanlarkhani, S.M. Mandani, A. Fattah-alhosseini, S.O. Gashti, Met. Mater. Int. **27**, 4463-4476 (2021).
[4] C. Zong, G. Zhu, W. Mao, Mater. Sci. Eng. A **563**, 1-7 (2013).
[5] S.I. Lee, J. Lee, B. Hwang, Mater. Sci. Eng. A **758**, 56-59 (2019).
[6] S.I. Lee, S.Y. Lee, J. Han, B. Hwang, Mater. Sci. Eng. A **742**, 334-343 (2019).
[7] S.I. Lee, S.Y. Lee, S.G. Lee, H.G. Jung, B. Hwang, Met. Mater. Int. **24**, 1221-1231 (2018).
[8] S.Y. Lee, S.I. Lee, B. Hwang, Mater. Sci, Eng. A **711**, 22-28 (2018).
[9] L.R. Jacobo, R. García-Hernández, V. H. López-Morelos, A. Contreras, Met. Mater. Int. **27**, 3750-3764 (2021).
[10] S.W. Lee, S.I. Lee, B. Hwang, Korean J. Met. Mater. **27**, 524-529 (2017).
[11] J.B. Ju, J.S. Lee, J.I. Jang, Mater. Lett. **61**, 5178-5180 (2007).
[12] M.S. Joo, D.W. Suh, H.K.D.H. Bhadeshia, ISIJ International **53**, 1305-1314 (2013).
[13] S.W. Lee, I.H. Im, B. Hwang, Korean J. Mater. Res. **28**, 702-708 (2018).
[14] Y.M. Kim, S.Y. Shin, H. Lee, B. Hwang, B.G. Park, S. Lee, N.J. Kim, Korean J. Met. Mater. **44**, 223-233 (2006).
[15] Y.M. Kim, S.Y. Shin, H. Lee, B. Hwang, S. Lee, N.J. Kim, Metall. Mater. Trans. A **38**, 1731-1742 (2007).
[16] S.Y. Shin, K.J. Woo, B. Hwang, S. Kim, S. Lee, Korean J. Met. Mater. **45**, 447-457 (2007).
[17] T.F.C. Hermenegildo, T.F.A. Santos, E.A. Torres, C.R.M. Afonso, A.J. Ramirez, Met. Mater. Int. **24**, 1120-1132 (2018).
[18] Y.M. Kim, H. Lee, N.J. Kim, Mater. Sci. Eng. A **478**, 361-370 (2008).
[19] M. Masoumi, L.F.G. Herculano, H.F.G. Abreu, Mater. Sci. Eng. A **639**, 550-558 (2015).
[20] H.K. Sung, D.H. Lee, S. Lee, H.S. Kim, Y. Ro, C.S. Lee, B. Hwang, S.Y. Shin, Metall. Mater. Trans. A **47**, 2726-2738 (2016).
[21] S.Y. Han, S.Y. Shin, S. Lee, N.J. Kim, J.H. Bae, K. Kim, Metall. Mater. Trans. A **41**, 329-340 (2010).
[22] Y.M. Kim, S.K. Kim, Y.J. Lim, N.J. Kim, ISIJ International **42**, 1571-1577 (2002).
[23] C.W. Choi, H.J. Koh, S. Lee, Metall. Mater. Trans. A **31**. 2669-2674 (2000).
[24] S.I. Lee, S.W. Lee, S.G. Lee, S. Lee, H.G. Jung, B. Hwang, Korean J. Met. Mater. **56**, 413-422 (2018).
[25] S. Nafish, M.A. Arafin, L. Collins, J. Szpunar, Mater. Sci. Eng. A **531**, 2-11 (2012).
[26] J.I. Omale, E.G. Ohaeri, J.A. Szpunar, M. Arafin, F. Fateh, Mater. Charact. **147**, 453-463 (2019).
[27] S.D. Bakshi, T. Dhande, N. Javed, K.N. Sasidhar, V. Sharma, M. Mukherjee, B. Ghosh, V.V. Mahashabde, Int. J. Press. Vessels Pip. **171**, 162-172 (2019).